Article

Not peer-reviewed version

Effect of Energy-Dependent Proton Irradiation in Thin-Film YBa2Cu3O7-δ Superconductor

Trevor Harrison , Joshua Kim , Katharina Cook , Hope Weeda , Joseph Fogt , Nolan Miles , Kyuil Cho *

Posted Date: 1 September 2025

doi: 10.20944/preprints202509.0088.v1

Keywords: high-temperature superconductor; Cuprates; YBCO; thin-film; proton irradiation; disorders; resistivity; Abrikosov-Gor'kov theory; d-wave

Article

Effect of Energy-Dependent Proton Irradiation in Thin-Film $YBa_2Cu_3O_{7-\delta}$ Superconductor

Trevor Harrison [1], Joshua Kim [1], Katharina Cook [1], Hope Weeda [1], Joseph Fogt [1], Nolan Miles [1] and Kyuil Cho [1,*]

Department of Physics, Hope College, Holland, MI 49423, USA
* Correspondence: cho@hope.edu

Abstract

The superconducting properties of $YBa_2Cu_3O_{7-\delta}$ thin-films were investigated by conducting 1.7 MeV proton irradiations with a total fluence of 2.64×10^{17} p/cm^2. The superconducting critical temperature (T_c) was reduced from 89.4 K to 10.1 K. The experimental procedure was similar to the previous study (0.6 MeV proton irradiation). We compared the effectiveness of T_c suppression by varying the proton energy from 0.6 to 1.7 MeV and found that in general both protons of 1.7 MeV and 0.6 MeV were effective in suppressing the T_c of YBCO. In particular, both results were consistent with the theoretical expectation (extended d-wave AG theory) when the zero-temperature London penetration depth (λ_0) = 215 nm is assumed for thin-film YBCO. For heavily irradiated cases (more than 80% T_c suppression), however, 1.7 MeV protons were more effective in suppressing T_c than 0.6 MeV protons. This can be understood by the fact that in thin-film limit, higher energy protons tend to produce less clustered point-defects while lower energy protons tend to create agglomeration of point-defects.

Keywords: high-temperature superconductor; Cuprates; YBCO; thin-film; proton irradiation; disorders; resistivity; Abrikosov-Gor'kov theory; d-wave

---

1. Introduction

The discovery of superconductivity in cuprate compounds in 1986 opened a new era of high-temperature superconductivity [1,2]. Due to their exceptional properties (high-T_c, J_c, and H_{c2}), they became important materials for novel technologies [3,4]. Among them, $YBa_2Cu_3O_{7-\delta}$ (YBCO) is one of the most studied compounds. While its Cooper pairing mechanism still remains under debate, it is widely accepted that the optimally-doped YBCO has $d_{x^2-y^2}$ wave pairing symmetry where the energy gap vanishes in nodal directions [5].

There are many different ways to investigate the pairing symmetry of a superconductor. One of the effective methods is to introduce artificial disorders into the crystal structure of the superconductor and study the response of its superconducting properties. According to Anderson's theorem, non-magnetic disorders are not effective in suppressing superconductivity of isotropic s-wave superconductors [6]. However, magnetic disorders are effective in suppressing the superconductivity of s-wave superconductors (so-called the Abrikosov-Gor'kov theory, or AG theory) [7]. In an anisotropic d-wave superconductor such as YBCO, non-magnetic disorders are also effective in suppressing the superconductivity [8]. Openov et al. developed a generalized AG theory to explain the effect of non-magnetic disorders on the property of d-wave superconductors [9].

Experimental confirmations of the generalized AG theory have been conducted through high-energy particle irradiation. Different types of particles generate different forms of defects [10]. Electron irradiation has been known to be most effective in the generation of point-like atomic-scale defects due to its low rest mass, resulting in a rapid suppression of superconductivity [11–14]. Other particles, such as protons and heavy ions, have previously been shown to be effective in creating cascading or columnar defects which have been known to be significantly less effective in suppressing superconductivity [15–18]. However, neither of these results (electron or others) successfully reproduced the theoretical expectations (generalized d-wave AG theory). Some results have reproduced similar behavior, but rely on a more qualitative analysis rather than direct quantitative agreement. These results were explained in terms of different quality of each sample, different plasma frequencies [8,19], different ratio between in-plane and out-of-plane defects [20], and different electron correlation [21–23]. In our previous study, we conducted 0.6 MeV proton irradiation of a thin-film YBCO superconductor using Hope College's particle accelerator (1.7 MV tandem Van de Graaff electrostatic accelerator) [24]. This experiment produced the results that are quantitatively closer to the theoretical expectation than any previous results. Therefore, we concluded that as the sample thickness approached the thin-film limit, the cascading defects produced by proton irradiation would become negligible, and the atomic point-like defects would dominate.

In this article, we conducted higher energy (1.7 MeV) proton irradiation in a YBCO thin-film superconductor and compared the result with the previous 0.6 MeV experiment. We found that in general, both 1.7 MeV and 0.6 MeV protons were equally effective in suppressing the superconductivity except for the most heavily irradiated cases (more than 80% T_c suppression). For the most heavily irradiated cases, the 1.7 MeV proton was more effective in suppressing T_c than the 0.6 MeV proton, indicating that the 0.6 MeV proton is more prone to create agglomeration of point defects than 1.7 MeV. Furthermore, we found that both results are consistent with the theoretical expectation when the larger London penetration depth value (λ_0 = 215 nm) was assumed for thin-film YBCO superconductors.

2. Material and Methods

2.1. YBCO Thin-Film and Resistance Measurements

The YBCO thin-film (≈567 nm thick) was epitaxially grown on a lanthanum aluminate ($LaAlO_3$, or LAO) substrate. The sample was originally fabricated as resonators in commercial microwave filters for wireless base stations [25]. This thin-film sample shows $T_c \approx 89.4$ K, indicating that its superconducting property is close to the bulk single-crystalline sample of $T_c \approx 93$ K [2]. This sample is of the same batch as the previous study with 0.6 MeV proton irradiation [24].

The in-plane resistance of the YBCO thin-film was measured using a standard four-probe technique as shown in Figure 1. The dimensions of the measured part of the sample are 1.835 ($\pm$ 0.014) mm $\times$ 0.263 ($\pm$ 0.0008) mm $\times$ 566.7 ($\pm$ 1.9) nm. Four electrical contacts made of fine gold wires were adhered to the thin film using silver paste.

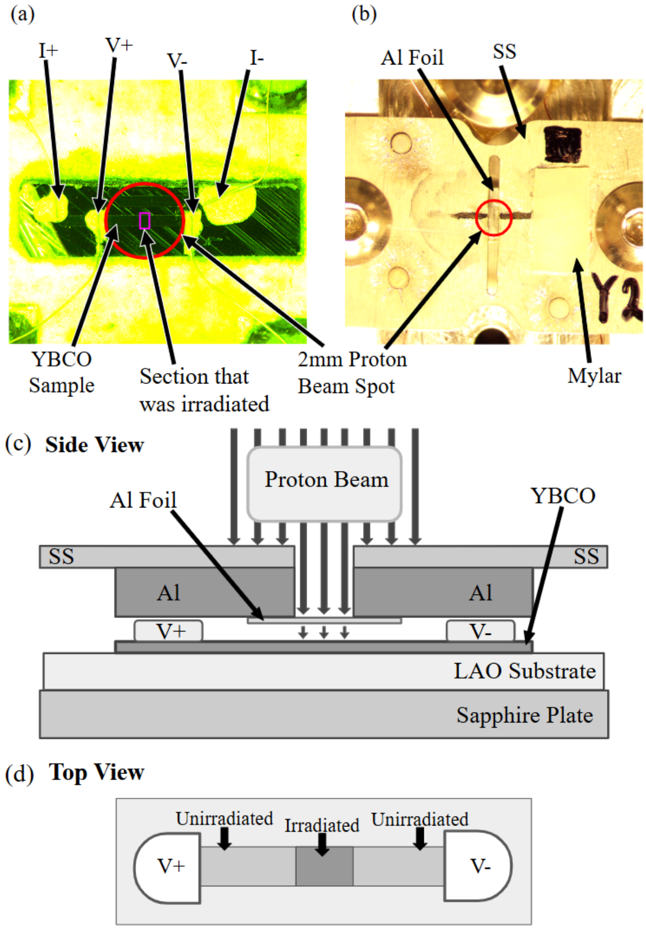

Figure 1. YBCO sample mounted in the sample holder. (a) The rectangle on the diagram denotes the section of YBCO that was irradiated. The circle on the diagram indicates the 2 mm diameter beam spot on the sample (b) A stainless steel (SS) beam shield was placed above the sample, reducing the beam width to exactly 0.5 mm. A Mylar scintillator is placed on the beam shield for calibration of the homogeneous 2 mm diameter proton beam. A 50 μm Al energy degrader is placed to reduce the beam energy from 2.85 MeV to 1.7 MeV. (c) Side view of the sample holder including the SS beam shield above the YBCO sample, which is grown on the LAO substrate mounted on a sapphire plate. (d) Top view of YBCO sample showing the portions of the unirradiated and irradiated parts of the sample. Proton irradiation is homogeneous in the irradiated section of the sample.

2.2. Energy Degrader and Homogeneous Proton Beam

The proton beam was produced by Hope College's particle accelerator (1.7 MV tandem Van de Graaff electrostatic accelerator) which is capable of generating proton beams of up to 3.4 MeV kinetic energy. The irradiation was performed at 6×10^{-8} torr at room temperature. This irradiation was conducted along the c-axis of the YBCO sample. 1.7 MeV proton beam was generated by using a 50 μm-thick aluminum energy degrader. Using SRIM calculation as shown in Figure 2, we confirmed that if a 2.85 MeV beam passes through a degrader of this thickness, the beam on our target would be 1.7 MeV. This degrader was held in place under the stainless-steel (SS) irradiation shield which shielded the entire sample from irradiation besides a 0.5 mm slit on the target area as seen in Figure 1(a-c). We tuned the beam to a 2 mm diameter beam spot on the Mylar strip atop the sample mount and the quadrupole magnets. We checked that this beam was homogeneous by capturing images of the beam spot and performing an intensity analysis. We tuned the beam until the intensity of the scintillator image was approximately 2 mm across with an even peak. We calibrated the image using the 2 mm by 2 mm square next to the Mylar scintillator as seen in Figure 1(b). This careful calibration was essential to ensuring a homogeneous proton beam. The irradiation was divided into 30-minute increments, during which we would measure the beam current and check the homogeneity of the beam. Using these current calculations, we estimated the fluences on target as shown in the results. The current on

Preprints.org (www.preprints.org) | NOT PEER-REVIEWED | Posted: 1 September 2025 doi:10.20944/preprints202509.0088.v1

target was kept to about 10 nA to avoid sample heating. During irradiation, we experienced some charge buildup issue in the sample. This resulted in fractures occurring along the silver paste line in the YBCO, which destroys the sample. We avoided this effect by grounding four electrical contacts to the metallic sample holder during the irradiation, which eliminated the rapid charge buildup and discharging issue.

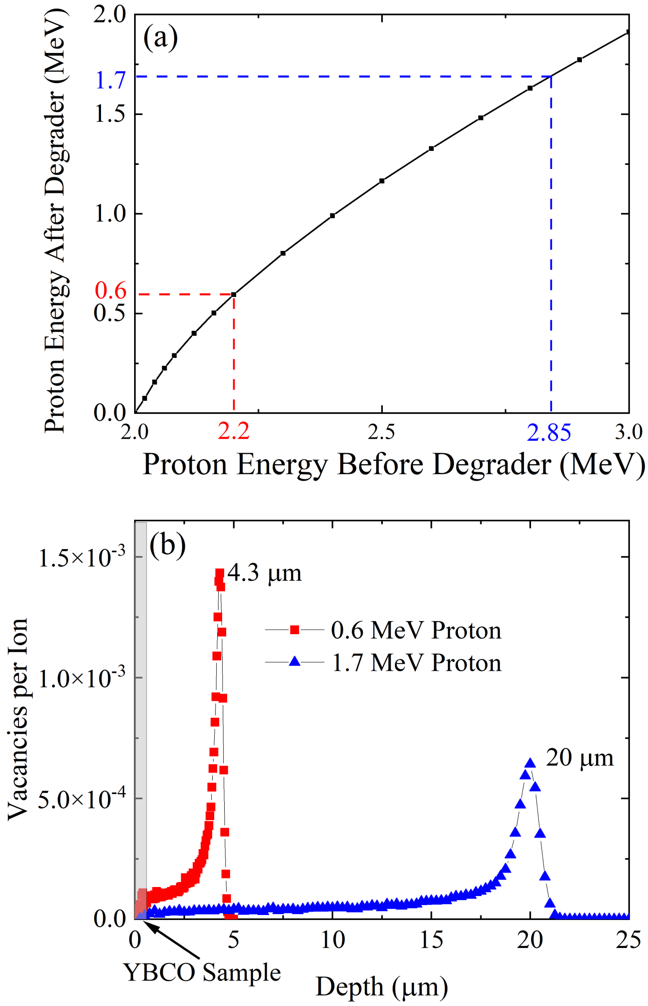

Figure 2. (a) The proton beam energy before and after the 50 μm Al energy degrader. The blue and red dotted lines denote the beam energies of the current (1.7 MeV) and previous experiments (0.6 MeV), respectively. These data are calculated using SRIM simulation [26]. (b) TRIM simulation results that show vacancies-per-ion along depth for 1.7 and 0.6 MeV protons. Implantation depths for 1.7 MeV and 0.6 MeV protons are about 20 μm and 4.3 μm, respectively. Since thickness of YBCO thin-film is 567 nm, the protons will be implanted into the LAO substrate. From the simulation, it is clear that a 0.6 MeV proton is about three times more effective in creating defects in YBCO thin-film than a 1.7 MeV proton.

3. Results and Discussion

Five resistance measurements and four 1.7 MeV proton irradiations were alternatively conducted in the same YBCO thin-film. The measured resistance is plotted in Figure 3 (a) in comparison to the previous study of 0.6 MeV proton irradiations (Figure 3 (b)). All of these data show two superconducting transitions except for the pristine cases. These double transitions occur since only part of the area in which the resistance was measured was irradiated as described in Figure 1 (d). The T_c of the unirradiated part does not change while the T_c of the irradiated part decreases with increasing fluence. The normal state resistance above T_c linearly increases upon irradiation following Matthiessen's rule. This increase indicates that the number of defects in the irradiated part of the sample increases gradually upon irradiation. The rate of T_c suppression with respect to the fluence is about three times larger

Preprints.org (www.preprints.org) | NOT PEER-REVIEWED | Posted: 1 September 2025 doi:10.20944/preprints202509.0088.v1

for 0.6 MeV proton irradiation than for 1.7 MeV proton irradiation (Figure 4(b)). This is because as we increase the energy of the proton beam, we simultaneously increase the implantation depth. The greater implantation depth means the less energy per proton is deposited into our thin-film sample. As shown in Figure 2(b), it is evident that the number of defects created in the thin-film YBCO sample is about three times smaller for 1.7 MeV protons than for 0.6 MeV protons. This is consistent with the fact that 1.7 MeV proton irradiation needs about three times more fluence than 0.6 MeV proton irradiation to achieve the similar T_c suppression as shown in Figure 4 (b). Figure 4(a) shows the broadening of superconducting transition upon irradiation. This broadening is caused by the spacing between aluminum energy degrader and the thin-film surface being about 0.5 - 0.7 mm. In the future, we plan to redesign the sample holder to decrease this spacing to 0.2 mm in order to minimize the broadening effect.

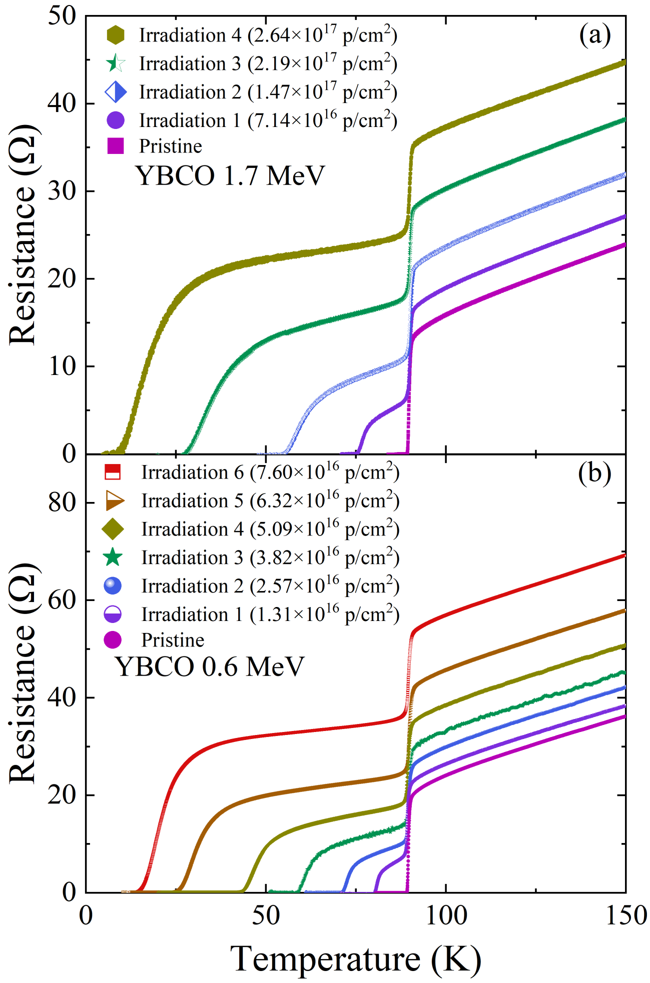

Figure 3. Temperature-dependent resistance data upon a series of (a) 1.7 MeV and (b) 0.6 MeV proton irradiations. The fluences shown in legends are initially measured by Faraday cup and corrected by using Rutherford-Back-Scattering calibration procedure [27]. For both cases, we see a linear increase in the normal-state resistance upon proton irradiations which is consistent with Matthiessen's rule.

 doi:10.20944/preprints202509.0088.v1

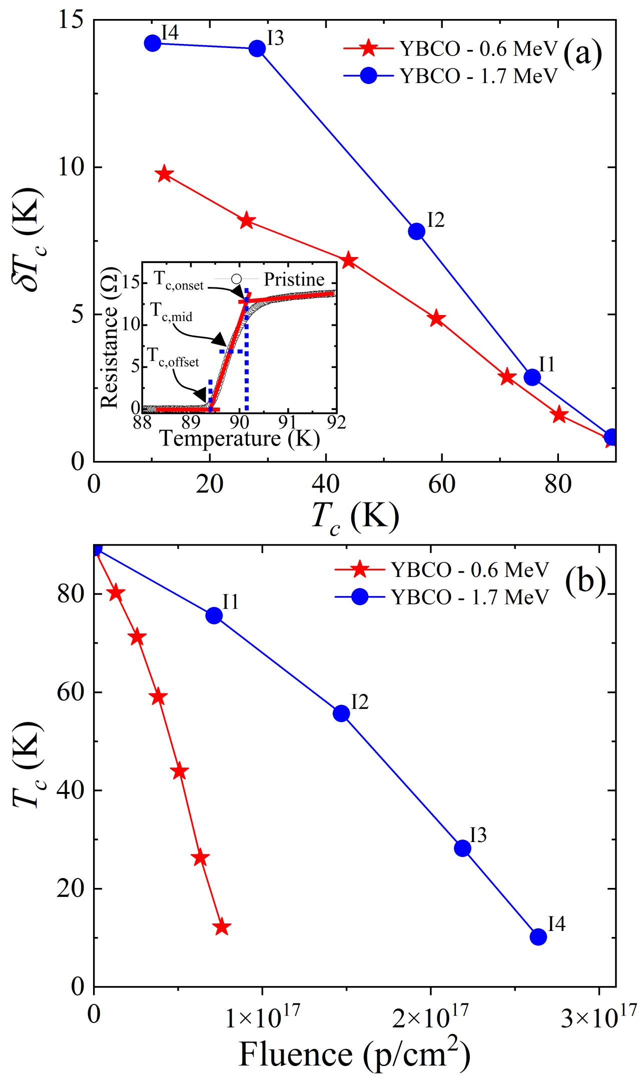

Figure 4. (a) Broadening of the superconducting transition ($\delta T_c = T_{c,onset} - T_{c,offset}$) for 1.7 MeV and 0.6 MeV proton irradiations. $T_{c,onset}$ and $T_{c,offset}$ are defined in the inset. The horizontal axis is the $T_{c,offset}$, and the vertical axis is the irradiation's associated broadening. We see much greater broadening in the 1.7 MeV irradiation. (b) $T_{c,offset}$ measured for various fluences on 0.6 MeV irradiated and 1.7 MeV irradiated samples. The 1.7 MeV proton beam requires about three times more fluence in order to suppress the superconductivity compared to the 0.6 MeV proton beam. This is consistent with TRIM simulation shown in Figure 2.

The increase in normal-state resistance is caused by the resistance increase in the irradiated part of the sample. Thus, we can convert the resistance increase to the resistivity increase by considering the volume of the irradiated part of the sample. Because the normal state resistance increases linearly across all temperature regions above the superconducting transition, the resistance value at 125 K was chosen to calculate the resistivity increase ($\Delta\rho_{125K}$).

According to Openov [19], the generalized AG theory for the case of the non-magnetic disorders in d-wave superconductors can be written as follows,

$$-ln(t_c) = \Psi(\frac{1}{2} + \frac{g}{2\,t_c}) - \Psi(\frac{1}{2}), \tag{1}$$

where t_c is T_c/T_{c0}, T_{c0} is the initial T_c before the disorders are added, and g is the dimensionless scattering rate. t_c asymptotically goes to zero as g approaches 0.28. Using the Drude model [28,29], g can also be written in terms of the residual resistivity (ρ_0) as follows,

$$g = \frac{\hbar\,\rho_0}{2\pi k_B \mu_0 T_{c0} \lambda_0^2}, \tag{2}$$

Preprints.org (www.preprints.org) | NOT PEER-REVIEWED | Posted: 1 September 2025 doi:10.20944/preprints202509.0088.v1

where ρ_0 is the residual resistivity at T = 0 K of the irradiated part of the YBCO sample, T_{c0} is the critical temperature of the pristine sample, and λ_0 is the zero-temperature London penetration depth of the pristine sample. Due to the high T_c of the YBCO sample, it is difficult to estimate the exact residual resistivity. If the normal state residual resistivity is very small, ρ_0 in Eq. 2 can be replaced by $\Delta\rho$. Indeed, the linear approximation of normal state resistivity in our previous study [24] suggests very small residual resistivity at T = 0 K ($\approx 8\ \mu\Omega cm$) and the current YBCO sample is almost identical to the previous sample as shown in Figure 7. By replacing ρ_0 in Eq. 2 with $\Delta\rho$, g can be rewritten as follows,

$$g \approx \frac{\hbar\, \Delta\rho_{125K}}{2\pi k_B \mu_0 T_{c0} \lambda_0^2}, \tag{3}$$

where $\Delta\rho_{125K}$ is the resistivity increase at T = 125 K of the irradiated part of the YBCO sample. This calculation requires a value for the London penetration depth, which we are not able to measure in our lab. Therefore, we surveyed experimental values of λ_0 from the previous studies, such as 1460 ± 150 Å [30], 1550 Å [31], 1990 ± 200 Å [32], and 2150 Å [33]. Among them, we used 2150 Å [33] for thin-film single-crystalline YBCO samples and 1405 ± 92 Å [34] for bulk single-crystalline YBCO samples in Figure 6. The YBCO single-crystallined thin-films on LAO substrate are structurally less perfect than YBCO bulk single crystals. Therefore, strong scattering of the charge carriers, characterized by the mean-free path (l), is expected to extend the penetration depth in thin-film samples similar to that predicted by Tinkham [35] for "dirty" superconductors. Thus, large λ_0 of 215 nm is reasonable for thin-film samples. For the purpose of comparison, we used both London penetration depth values of 140.5 nm and 215 nm to plot our results in Figure 5. When λ_0 = 215 nm is used, both 1.7 MeV and 0.6 MeV results closely follow the theoretical expectation. However,the heavily irradiated results (more than 80% T_c suppression) start deviating from the theoretical expectation. This indicates a development of extended defects where the nearby point defects agglomerate at high fluence as mentioned by Wu *et al.* [15]. For the most heavily irradiated cases, furthermore, T_c suppression upon 0.6 MeV proton irradiation is not as effective as 1.7 MeV proton irradiation. It suggests that lower-energy protons are prone to create a cluster of point defects even in the thin-film limit than the higher-energy protons.

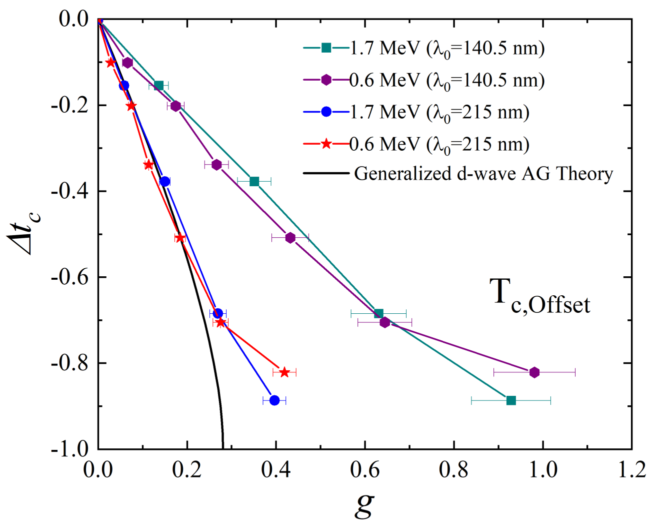

Figure 5. Normalized T_c ($\Delta t_c = (T_c - T_{c0})/T_{c0}$) as a function of g (dimensionless scattering rate) upon 1.7 MeV and 0.6 MeV proton irradiation. Since g depends on the London penetration depth (λ_0), we used two values commonly used for bulk single-crystalline (140.5 nm) and thin-film YBCO (214 nm). When λ_0 = 215 nm is used, both 1.7 and 0.6 MeV proton irradiation results closely follow the theoretical expectation. For the heavily irradiated cases (more than 60 % T_c suppression), both results start deviating from the theoretical expectation. Particularly for the most heavily irradiated cases (more than 80 % T_c suppression) there is a clear difference between 1.7 MeV and 0.6 MeV irradiation.

It is evident that the agglomeration is more significant in 0.6 MeV proton irradiation than 1.7 MeV proton irradiation.

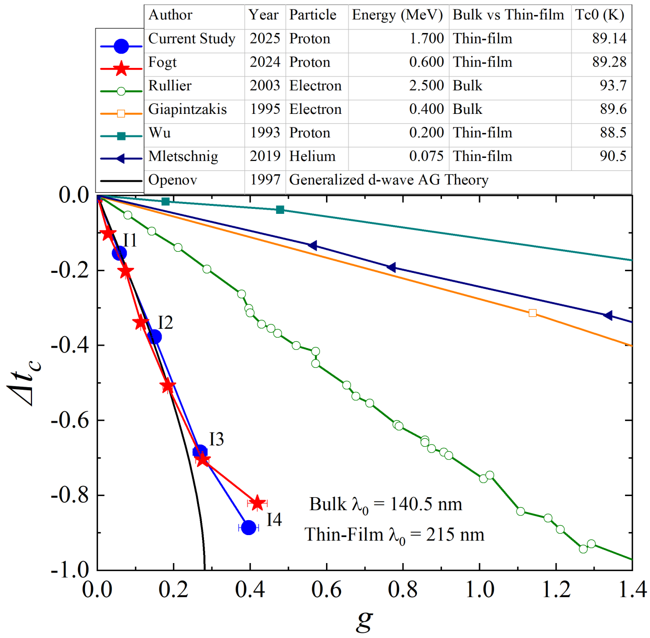

Figure 6. Normalized T_c ($\Delta t_c = (T_c - T_{c0})/T_{c0}$) as a function of g (dimensionless scattering rate) for previous studies and current 1.7 MeV proton irradiation study [10–12,15,24].

Figure 6 compares the relation between T_c and g of the current study with previous irradiation studies [10–12,15,24] and theoretical expectation [19]. Note that different penetration depth values are used for bulk single crystals and thin-film single crystals. The current proton irradiation study is the one that most agrees with the theoretical expectation. In particular, it is surprising that the current proton irradiation is more effective in suppressing superconductivity than the electron irradiation. This can be partially understood that the dominant form of defects caused by proton irradiations shifts from cascade defects to atomic-size point-defects as the sample thickness reaches the thin-film limit; i.e., the implantation depth of the proton becomes much longer relative to the sample thickness. However, further investigation is needed to fully understand it.

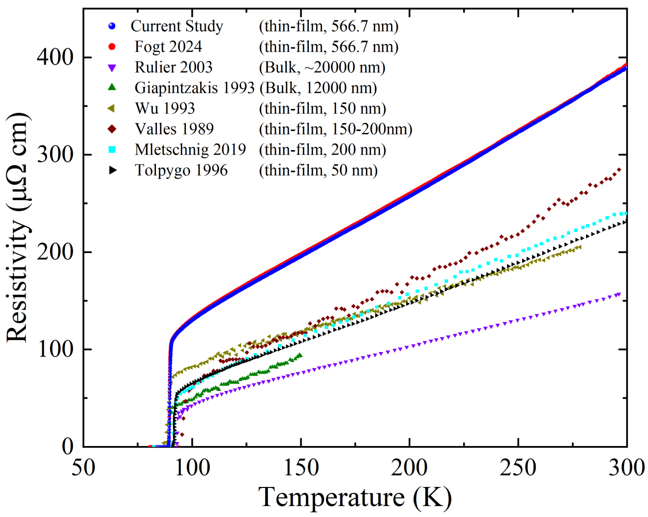

Figure 7. The pristine resistivity of the 0.6 MeV and 1.7 MeV samples. There is little to no difference in the sample resistivity indicating the samples are nearly identical. Normal state resistivity is higher in the current YBCO study than previous studies.

4. Conclusions

We conducted 1.7 MeV proton irradiation in a YBCO thin film and compared the result with the previous study (0.6 MeV proton irradiation). We found that both 1.7 MeV and 0.6 MeV irradiations were effective in suppressing superconductivity. For the most heavily irradiated cases (more than 80 % T_c suppression), 0.6 MeV irradiation was less effective in suppressing the superconductivity than 1.7 MeV. This indicates that 0.6 MeV irradiation produced more agglomeration of point-defects for the heavily irradiated cases. Furthermore, when λ_0 = 215 nm is assumed, both 1.7 MeV and 0.6 MeV results were consistent with the theoretical expectation except for the most heavily irradiated cases.

Author Contributions: Conceptualization and sample preparation, K.Cho; proton irradiation and resistance measurement, T.H., J.K. K.Cook, H.W., J.F., and N.M.; data analysis and calculation, T.H., J.K. K.Cook, H.W., J.F., and N.M.; writing—original draft preparation and review, T.H., J.K. K.Cook, H.W., J.F., N.M., K.Cho. All authors have read and agreed to the published version of the manuscript.

Funding: The laboratory facilities are supported by the National Science Foundation under grants NSF PHYS-0319523 and PHYS-2209138. The research reported in this publication was supported in part by funding provided by the National Aeronautics and Space Administration (NASA), under award number 80NSSC20M0124, Michigan Space Grant Consortium (MSGC).

Data Availability Statement: The data presented in this study are available on reasonable request from the corresponding author.

Acknowledgments: We thank Paul DeYoung and Andrew Bunnell for assisting us in operating the particle accelerator. We thank David Daugherty for assisting us in designing new sample mounts. We thank Stephen Remillard for providing YBCO samples.

Conflicts of Interest: The authors declare no conflicts of interest.

References

1. Bednorz, J.G.; Mueller, K.A. Possible high Tc superconductivity in the barium-lanthanum-copper-oxygen system. *Z. Phys. B: Condens. Matter* **1986**, *64*, 189–93. https://doi.org/10.1007/BF01303701.
2. Wu, M.K.; Ashburn, J.R.; Torng, C.J.; Hor, P.H.; Meng, R.L.; Gao, L.; Huang, Z.J.; Wang, Y.Q.; Chu, C.W. Superconductivity at 93 K in a new mixed-phase Y-Ba-Cu-O compound system at ambient pressure. *Phys. Rev. Lett.* **1987**, *58*, 908–910. https://doi.org/10.1103/PhysRevLett.58.908.
3. Hahn, S.; Kim, K.; Kim, K.; Hu, X.; Painter, T.; Dixon, I.; Kim, S.; Bhattarai, K.R.; Noguchi, S.; Jaroszynski, J.; et al. 45.5-tesla direct-current magnetic field generated with a high-temperature superconducting magnet. *Nature* **2019**, *570*, 496–499. https://doi.org/10.1038/s41586-019-1293-1.
4. Molodyk, A.; Samoilenkov, S.; Markelov, A.; Degtyarenko, P.; Lee, S.; Petrykin, V.; Gaifullin, M.; Mankevich, A.; Vavilov, A.; Sorbom, B.; et al. Development and large volume production of extremely high current density YBa2Cu3O7 superconducting wires for fusion. *Scientific Reports* **2021**, *11*, 2084. https://doi.org/10.1038/s41598-021-81559-z.
5. Tsuei, C.C.; Kirtley, J.R. Pairing symmetry in cuprate superconductors. *Rev. Mod. Phys.* **2000**, *72*, 969–1016. https://doi.org/10.1103/RevModPhys.72.969.
6. Anderson, P.W. Theory of dirty superconductors. *Journal of Physics and Chemistry of Solids* **1959**, *11*, 26–30. https://doi.org/10.1016/0022-3697(59)90036-8.
7. Abrikosov, A.A.; Gor'kov, L.P. Contribution to the theory of superconducting alloys with paramagnetic impurities. *Zh. Eksp. Teor. Fiz. (Sov. Phys. JETP 12, 1243 (1961))* **1960**, *39*, 1781.
8. Radtke, R.J.; Levin, K.; Schüttler, H.B.; Norman, M.R. Predictions for impurity-induced T_c suppression in the high-temperature superconductors. *Phys. Rev. B* **1993**, *48*, 653–656. https://doi.org/10.1103/PhysRevB.48.653.
9. Openov, L.A. Combined effect of nonmagnetic and magnetic scatterers on the critical temperatures of superconductors with different anisotropies of the gap. *Journal of Experimental and Theoretical Physics Letters* **1997**, *66*, 661–667. https://doi.org/10.1134/1.567576.
10. Mletschnig, K.; Lang, W. Nano-patterning of cuprate superconductors by masked He+ ion irradiation: 3-dimensional profiles of the local critical temperature. *Microelectronic Engineering* **2019**, *215*, 110982. https://doi.org/https://doi.org/10.1016/j.mee.2019.110982.

11. Rullier-Albenque, F.; Alloul, H.; Tourbot, R. Influence of Pair Breaking and Phase Fluctuations on Disordered High T_c Cuprate Superconductors. *Phys. Rev. Lett.* **2003**, *91*, 047001. https://doi.org/10.1103/PhysRevLett.91.047001.
12. Giapintzakis, J.; Ginsberg, D.M.; Kirk, M.A. Determination of the symmetry of the superconducting pairing state and formation of a low-temperature normal metallic state in YBCO by electron irradiation. *Technical Report* **1995**. https://doi.org/doi:10.2172/510599.
13. Cho, K.; Kończykowski, M.; Teknowijoyo, S.; Tanatar, M.A.; Liu, Y.; Lograsso, T.A.; Straszheim, W.E.; Mishra, V.; Maiti, S.; Hirschfeld, P.J.; et al. Energy gap evolution across the superconductivity dome in single crystals of $Ba_{1-x}K_xFe_2As_2$. *Science Advances* **2016**, *2*, e1600807. https://doi.org/10.1126/sciadv.1600807.
14. Cho, K.; Kończykowski, M.; Teknowijoyo, S.; Ghimire, S.; Tanatar, M.A.; Mishra, V.; Prozorov, R. Intermediate scattering potential strength in electron-irradiated $YBa_2Cu_3O_{7-\delta}$ from London penetration depth measurements. *Phys. Rev. B* **2022**, *105*, 014514. https://doi.org/10.1103/PhysRevB.105.014514.
15. Wu, J.Z.; Yu, N.; Chu, W.K. Anisotropy of the ion-beam radiation effect in $YBa_2Cu_3O_{7-\delta}$ (110) thin films. *Phys. Rev. B* **1993**, *48*, 9929–9931. https://doi.org/10.1103/PhysRevB.48.9929.
16. Torsello, D.; Fracasso, M.; Gerbaldo, R.; Ghigo, G.; Laviano, F.; Napolitano, A.; Iebole, M.; Cialone, M.; Manca, N.; Martinelli, A.; et al. Proton Irradiation Effects on the Superconducting Properties of Fe(Se,Te) Thin Films. *IEEE Transactions on Applied Superconductivity* **2022**, *32*, 1–5. https://doi.org/10.1109/TASC.2021.3136135.
17. Konczykowski, M.; Rullier-Albenque, F.; Yacoby, E.R.; Shaulov, A.; Yeshurun, Y.; Lejay, P. Effect of 5.3-GeV Pb-ion irradiation on irreversible magnetization in Y-Ba-Cu-O crystals. *Phys. Rev. B* **1991**, *44*, 7167–7170. https://doi.org/10.1103/PhysRevB.44.7167.
18. Nakajima, Y.; Tsuchiya, Y.; Taen, T.; Tamegai, T.; Okayasu, S.; Sasase, M. Enhancement of critical current density in Co-doped $BaFe_2As_2$ with columnar defects introduced by heavy-ion irradiation. *Phys. Rev. B* **2009**, *80*, 012510. https://doi.org/10.1103/PhysRevB.80.012510.
19. Openov, L.A. Critical temperature of an anisotropic superconductor containing both nonmagnetic and magnetic impurities. *Phys. Rev. B* **1998**, *58*, 9468–9478. https://doi.org/10.1103/PhysRevB.58.9468.
20. Graser, S.; Hirschfeld, P.J.; Zhu, L.Y.; Dahm, T. T_c suppression and resistivity in cuprates with out of plane defects. *Phys. Rev. B* **2007**, *76*, 054516. https://doi.org/10.1103/PhysRevB.76.054516.
21. Garg, A.; Randeria, M.; Trivedi, N. Strong correlations make high-temperature superconductors robust against disorder. *Nature Physics* **2008**, *4*, 762–765. https://doi.org/10.1038/nphys1026.
22. Kemper, A.F.; Doluweera, D.G.S.P.; Maier, T.A.; Jarrell, M.; Hirschfeld, P.J.; Cheng, H.P. Insensitivity of d-wave pairing to disorder in the high-temperature cuprate superconductors. *Phys. Rev. B* **2009**, *79*, 104502. https://doi.org/10.1103/PhysRevB.79.104502.
23. Tang, S.; Dobrosavljević, V.; Miranda, E. Strong correlations generically protect d-wave superconductivity against disorder. *Phys. Rev. B* **2016**, *93*, 195109. https://doi.org/10.1103/PhysRevB.93.195109.
24. Fogt, J.; Weeda, H.; Harrison, T.; Miles, N.; Cho, K. Effect of Proton Irradiation on Thin-Film YBa2Cu3O7 Superconductor. *Materials* **2024**, *17*, 4601. https://doi.org/10.3390/ma17184601.
25. Remillard, S.K.; Kirkendall, D.; Ghigo, G.; Gerbaldo, R.; Gozzelino, L.; Laviano, F.; Yang, Z.; Mendelsohn, N.A.; Ghamsari, B.G.; Friedman, B.; et al. Microwave nonlinearity and photoresponse of superconducting resonators with columnar defect micro-channels. *Superconductor Science and Technology* **2014**, *27*, 095006. https://doi.org/10.1088/0953-2048/27/9/095006.
26. Ziegler, J.F.; Ziegler, M.; Biersack, J. SRIM– The stopping and range of ions in matter. *Nuclear Instruments and Methods in Physics Research B*, *268*, 1818–1823.
27. Miles, N.; Fogt, J.; Harrison, T.; Weeda, H.; Bunnell, A.; A. DeYoung, P.; Cho, K. Correcting Faraday Cup Measurements with Rutherford Backscattering Spectroscopy. *Journal of Undergraduate Research in Physics and Astronomy* **2025**, *xx*, xxxxx.
28. Prozorov, R.; Kończykowski, M.; Tanatar, M.A.; Thaler, A.; Bud'ko, S.L.; Canfield, P.C.; Mishra, V.; Hirschfeld, P.J. Effect of Electron Irradiation on Superconductivity in Single Crystals of $Ba(Fe_{1-x}Ru_x)_2As_2$ ($x = 0.24$). *Phys. Rev. X* **2014**, *4*, 041032. https://doi.org/10.1103/PhysRevX.4.041032.
29. Cho, K.; Kończykowski, M.; Teknowijoyo, S.; Tanatar, M.A.; Prozorov, R. Using electron irradiation to probe iron-based superconductors. *Superconductor Science and Technology* **2018**, *31*, 064002. https://doi.org/10.1088/1361-6668/aabfa8.
30. Prozorov, R.; Giannetta, R.W.; Carrington, A.; Fournier, P.; Greene, R.L.; Guptasarma, P.; Hinks, D.G.; Banks, A.R. Measurements of the absolute value of the penetration depth in high-Tc superconductors using a low-Tc superconductive coating. *Applied Physics Letters* **2000**, *77*, 4202–4204, [https://pubs.aip.org/aip/apl/article-pdf/77/25/4202/18554366/4202_1_online.pdf]. https://doi.org/10.1063/1.1328362.

 doi:10.20944/preprints202509.0088.v1

31. Bernhard, C.; Niedermayer, C.; Binninger, U.; Hofer, A.; Wenger, C.; Tallon, J.L.; Williams, G.V.M.; Ansaldo, E.J.; Budnick, J.I.; Stronach, C.E.; et al. Magnetic penetration depth and condensate density of cuprate high-T_c superconductors determined by muon-spin-rotation experiments. *Phys. Rev. B* **1995**, *52*, 10488–10498. https://doi.org/10.1103/PhysRevB.52.10488.
32. Djordjevic, S.; de Vaulchier, L.A.; Bontemps, N.; Vieren, J.P.; Guldner, Y.; Moffat, S.; Preston, J.; Castel, X.; Guilloux-Viry, M.; Perrin, A. Low temperature penetration depth and the effect of quasi-particle scattering measured by millimeter wave transmission in YBa2Cu3O7$-\delta$ thin films. *The European Physical Journal B - Condensed Matter and Complex Systems* **1998**, *5*, 847–858. https://doi.org/10.1007/s100510050511.
33. Zaitsev, A.G.; Schneider, R.; Linker, G.; Ratzel, F.; Smithey, R.; Schweiss, P.; Geerk, J.; Schwab, R.; Heidinger, R. Microwave measurements of the absolute London penetration depth in double-sided YBa2Cu3O7—x thin films on sapphire. *Review of Scientific Instruments* **2002**, *73*, 335–344, [https://pubs.aip.org/aip/rsi/article-pdf/73/2/335/19030654/335_1_online.pdf]. https://doi.org/10.1063/1.1435842.
34. Bonn, D.A.; Liang, R.; Riseman, T.M.; Baar, D.J.; Morgan, D.C.; Zhang, K.; Dosanjh, P.; Duty, T.L.; MacFarlane, A.; Morris, G.D.; et al. Microwave determination of the quasiparticle scattering time in $YBa_2Cu_3O_{6.95}$. *Phys. Rev. B* **1993**, *47*, 11314–11328. https://doi.org/10.1103/PhysRevB.47.11314.
35. Tinkham, M. *Introduction to Superconductivity*; McGraw Hill, 1996.